

Quantitative time-resolved measurement of membrane protein–ligand interactions using microcantilever array sensors

Thomas Braun^{1†}, Murali Krishna Ghatkesar^{2†}, Natalija Backmann³, Wilfried Grange¹, Pascale Boulanger⁴, Lucienne Letellier⁴, Hans-Peter Lang³, Alex Bietsch³, Christoph Gerber³ and Martin Hegner^{1*}

Membrane proteins are central to many biological processes, and the interactions between transmembrane protein receptors and their ligands are of fundamental importance in medical research. However, measuring and characterizing these interactions is challenging. Here we report that sensors based on arrays of resonating microcantilevers can measure such interactions under physiological conditions. A protein receptor—the FhuA receptor of *Escherichia coli*—is crystallized in liposomes, and the proteoliposomes then immobilized on the chemically activated gold-coated surface of the sensor by ink-jet spotting in a humid environment, thus keeping the receptors functional. Quantitative mass-binding measurements of the bacterial virus T5 at subpicomolar concentrations are performed. These experiments demonstrate the potential of resonating microcantilevers for the specific, label-free and time-resolved detection of membrane protein–ligand interactions in a micro-array format.

Membrane proteins have an important role in many biological processes, including the transport of matter, energy conversion, communication and the interaction of cells with their environment. Indeed, membrane proteins are the most important target for present-day drug discovery programmes, with half of all marketed drugs affecting membrane proteins called G-protein-coupled receptors (GPCRs)¹.

Unfortunately, the special architecture of transmembrane proteins (which is a result of the amphiphilic nature of most biological (lipid) membranes) makes it challenging to work with them², and makes it difficult to obtain structural and functional data. However, given their medical importance, there is a need to find new ways to study membrane proteins under physiological conditions, preferably methods that are label-free and enable real-time measurements in a ‘functional micro-array’ format³.

Recently, new sensor technologies based on microcantilevers have been developed^{4,5}. Two changes occur when analyte molecules bind to immobilized receptors on the surface of a cantilever: first, a surface stress-induced bending of the cantilever (static mode) occurs, and second, there is a change in the resonance frequency of the cantilever caused by the change in mass (dynamic mode).

Static mode detection has been established to be a sensitive label-free method for real-time detection of biomolecular interactions in air and liquid^{6–11}. It also represents a new method for monitoring conformational changes of immobilized molecules upon binding of analytes^{12,13}.

Dynamic mode measurements performed in vacuum or humid air have enabled the mass detection of a single virus particle¹⁴ and a bacterium cell¹⁵, as well as the monitoring of the growth of microorganisms on cantilever surfaces in humid air^{16,17}. However, real-time dynamic detection of biological ligands binding to receptors

is more challenging because it happens in a liquid physiological environment. The binding of biotinylated beads to streptavidin receptors has been detected in proof-of-concept experiments^{18,19}. The experiments of Burg and colleagues¹⁹ are an excellent demonstration of the miniaturization of sensors (with the sample flowing through channels inside the cantilever as it vibrates in a vacuum), although they were not performed in an array format (and did not, therefore, permit differential sensing). This technique enabled measurements of the binding of antibodies to antigens or weighing the mass of individual bacteria or gold particles with high sensitivity. However, real-time sensing of bio-ligands binding to membranes on cantilever arrays in liquid using the dynamic mode has not yet been established.

The detection of viruses present in biological samples such as serum is of high importance in medical diagnostics. Common indirect assay procedures include the detection and amplification of their genetic material with real-time polymerase chain reactions. An assay that directly detects viral binding to membranes is still not available^{20,21}. In the present study, we demonstrate the application of the dynamic mode method for virus detection in liquid using the model system of the complete *E. coli* outer transmembrane protein FhuA ($M_w = 78.9$ kDa)²².

Besides its physiological function as a specific membrane transporter of the siderophore (iron-chelating molecule) ferrichrome, FhuA is used as a receptor by numerous other effectors, which are mostly harmful to bacteria. Among them is the bacteriophage virus T5, which is a lytic phage. The binding site of the phage is different from that of ferrichrome^{23,24} and is accompanied by large energetic and structural changes, leading to cell penetration by a needle and subsequent DNA injection²³. Subsequently, T5 phages break up the infected cells after replication of their virus particles.

¹School of Physics and Centre for Research on Adaptive Nanostructures and Nanodevices (CRANN), Naughton Institute, Trinity College Dublin, Dublin 2, Ireland, ²California Institute of Technology, Pasadena, California 91107, USA, ³National Centre of Competence for Research in Nanoscience, Institute of Physics, University of Basel, Klingelbergstrasse 82, 4056 Basel, Switzerland, ⁴Institut de Biochimie et de Biophysique Moléculaire et Cellulaire, UMR CNRS 8619, Université Paris-Sud XI, 91405 Orsay, France; [†]These authors contributed equally to this work; *e-mail: Martin.Hegner@tcd.ie

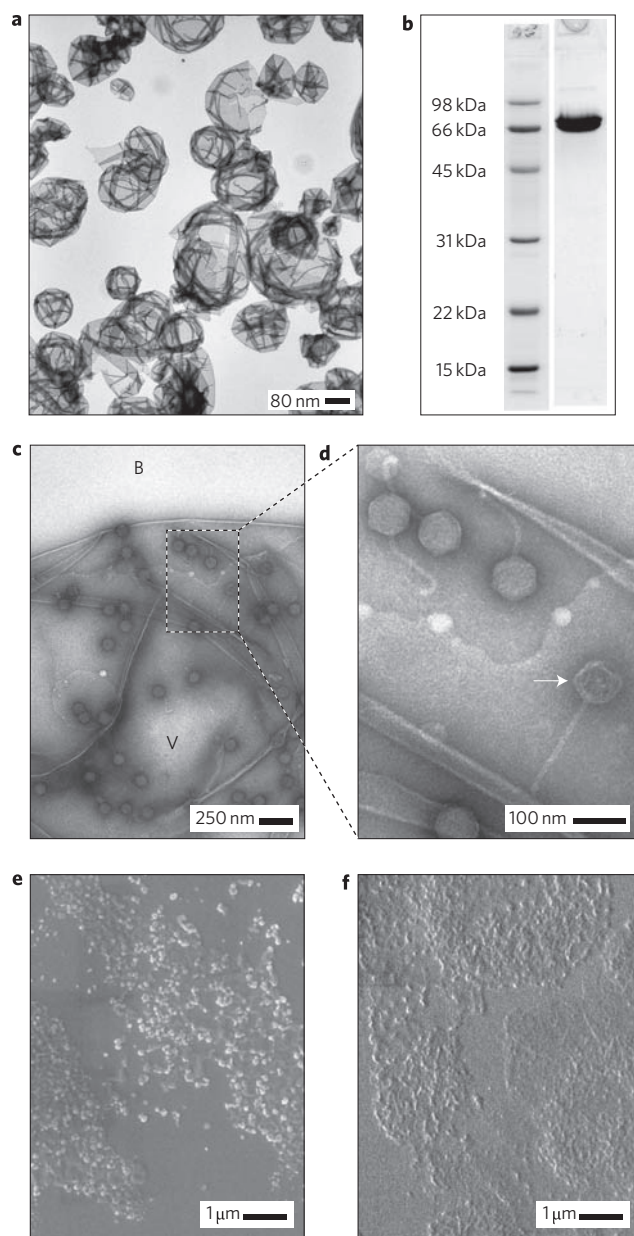


Figure 1 | Preparation of FhuA receptors for cantilever functionalization. **a**, TEM image of reconstituted FhuA-proteoliposomes. **b**, Coomassie-stained SDS-PAGE of reconstituted FhuA-protein (right lane), with molecular mass markers shown in the left lane. **c**, Binding of T5 phages to FhuA-containing vesicles (V) in solution (TEM). The background (carbon film) is labelled B. **d**, Magnification of the region indicated in **c**. The arrow indicates the empty head of a phage, which has most probably already injected the DNA into a vesicle. **e**, Binding of T5 phage to FhuA-containing proteoliposomes immobilized on a gold interface by means of a di-thio-bis-succinimidyl-undecanoate (DSU) crosslinker (scanning electron microscopy, SEM, image): gold-coated cantilevers were pre-functionalized with a self-assembled monolayer of DSU by immersion in 1 mM DSU solution in dioxan. **f**, Binding of T5 phages to FhuA-containing vesicles physisorbed on gold cantilever interfaces (SEM): experiments were performed as described in **e**, but without the pre-functionalization with the DSU layer. The immobilization of FhuA-proteoliposomes in **e** and **f** was performed in batch and not by ink-jet spotting.

FhuA-protein was reconstituted into liposomes and attached in a functional form to the gold-coated side of cantilevers using thiol crosslinking chemistry. The specific binding of T5 virus

particles (estimated $M_w = 7 \times 10^7$ Da)²⁵ on FhuA-protein was measured. All experiments were performed in a functional microarray format, allowing differential measurements of the sensing (FhuA-functionalized and casein-blocked) and reference (casein-functionalized only) cantilevers, in parallel, under the same physiological conditions. This allowed the sensitivity of the measurements to be improved when temperature drifts or non-specific binding were likely. (See Supplementary Information, Fig. S1, for an overview of the complete experimental workflow.)

Receptor preparation, stabilization and functionality test

FhuA-protein, solubilized and purified in the detergent *n*-octyl- β -D-glucopyranoside²⁶, was reconstituted in *E. coli*-derived lipids by dialysis^{27,28}. Figure 1a shows a transmission electron microscopy (TEM) image of the reconstituted material. Depending on the value of the lipid to protein weight/weight ratio (LPR), we observed small vesicles with a diameter of <200 nm (LPR > 0.5) or large vesicles with a diameter of >200 nm (LPR < 0.5). With a LPR of about 0.1, sheets of vesicles were instead obtained (these reconstitutions were not used for sensor functionalization). Depending on the LPR and the reconstitution experiment, the vesicles revealed partial (1 to 2 diffraction orders) crystallinity, or high crystallinity in the case of sheets, in the power spectra (data not shown). Figure 1b shows a sodium dodecyl sulphate-polyacrylamide gel electrophoresis (SDS-PAGE) of the reconstituted material. The strong band at ~ 70 kDa corresponds to the nominal molecular weight of FhuA, indicating that the protein was inserted into the vesicles. Further binding experiments were performed with FhuA reconstituted in pure vesicles rather than in sheets.

Before using the FhuA-containing proteoliposomes for cantilever measurements, we tested their ability to bind T5 phages in solution. The results were visualized using TEM. The phage-binding assay revealed a specific interaction between the virus particles and FhuA-protein-containing vesicles (Fig. 1c)²³, whereas only a few unbound viruses were observed in the background. The more detailed Fig. 1d shows the binding of the phage baseplate and the ample flexibility of the phage tail (see also Supplementary Information). Some phages, like the one indicated by an arrow in Fig. 1d, injected the DNA into the vesicle as demonstrated previously²⁹. Thus, these images confirmed the functionality of the reconstituted FhuA-proteins.

Measurements of biomolecular interactions with sensors require the ability to control the stability and activity of immobilized receptor molecules on the sensor interface. We tested the attachment and functionality of FhuA-proteoliposomes immobilized on gold-coated cantilever arrays using T5 phages as reporters. These bacterial viruses are sensitive to the general architecture of the protein³⁰. As such, these viruses not only provide evidence for the presence of the membrane proteins (as would antibodies), but also directly test their functionality. To this end, FhuA-containing proteoliposomes were either physisorbed directly on gold surfaces or attached to them covalently using a crosslinking monolayer of di-thio-bis-succinimidyl-undecanoate (DSU)³¹ molecules. After subsequent in-batch incubation of cantilevers in a T5 phage suspension, the results were visualized by scanning electron microscopy (SEM). We detected octahedral structures with the size of T5 heads only on the gold surface pre-functionalized with the DSU monolayer (Fig. 1e). When the proteoliposomes were adsorbed directly on the gold support, we observed only vesicle-like structures but no viral capsids (Fig. 1f). This suggests that direct adsorption of the proteoliposomes on the gold surface inactivates FhuA. In contrast, the protecting DSU layer between the gold and the proteoliposomes maintains the ability of membrane-incorporated FhuA-protein to bind phages. However, the in-batch functionalization of sensors was inefficient in two ways: it consumed a lot of biological material, and only a small portion of the interface revealed FhuA

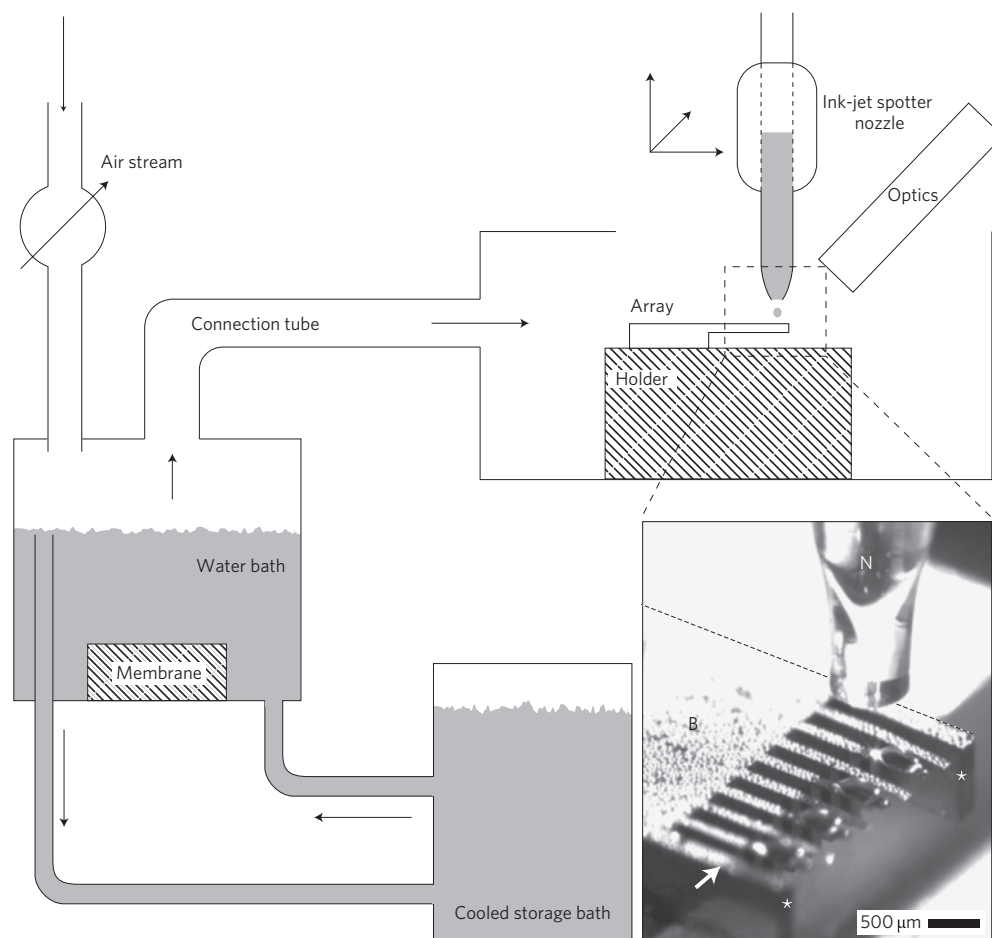


Figure 2 | Humidity chamber for functionalization of cantilevers with membrane proteins. The cantilever array is placed on a temperature-controlled (peltier) cantilever holder. The ink-jet spotter nozzle is used to spot droplets (~ 0.1 nl) on the cantilever surface and can be moved in all directions. The functionalization procedure is monitored by a charge-coupled device (CCD) camera through magnifying optics. To prevent drying of the biological functionalization layer, small water droplets are generated by a piezoelement-driven membrane placed in a water bath. The water of the bath is continuously exchanged by pumping from a cooled storage bath. The vapour generated above the humidifying bath is transported in a regulated air stream through a connection tube to the functionalization chamber with the cantilever array. The inset shows the nozzle N and a cantilever array as seen after functionalization through the camera. An arrow marks the hinge of the cantilever beam. The small water droplets on the base of the cantilever array B are generated in the humidity chamber. Every second cantilever is membrane protein functionalized (large drops). Note that the spotter nozzle N wets the upper interface selectively. The asterisks mark the protection bars at the side of the cantilevers. The profile of the chip body is indicated by a dotted line. Scale bar, 500 μm .

vesicles. To overcome these limitations, we have used an ink-jet spotter to directly functionalize the cantilevers (see below).

Cantilever functionalization by ink-jet spotting

The functionalization of the upper side of the DSU-prefunctionalized cantilevers was performed using an ink-jet spotter dispensing ten droplets (0.1 nl; distance between droplets, 50 μm) of proteoliposome-containing buffer on every second cantilever. To prevent drying of the spotted droplets (which could lead to a denaturation of proteins), we designed a humidity chamber to keep the cantilever surfaces wet for at least 30 min at a relative humidity of $>95\%$ (Fig. 2). In order to inhibit condensation of the humidity at the spotter nozzle, the setup was temperature-controlled at two points, at the water bath with the mist generator and at the cantilever holder itself. With additional control of the air stream, the conditions in the functionalization chamber could be precisely regulated, allowing excellent control of the wetting of the cantilever surface. In this way, the upper surface of the cantilever may be selectively functionalized with native biomolecules, allowing incubation times of up to 1 h.

After immobilization of FhuA–proteoliposomes (Fig. 3a), the complete array (positive and reference cantilevers) was immersed in a casein solution to block the remaining unspecific binding sites. Casein is widely used to prevent unspecific binding in molecular biological applications and does not block receptor ligand interaction³². This functionalization procedure therefore resulted in an array containing four sensing cantilevers covered with FhuA–proteoliposomes and four reference cantilevers, covered with casein only. Note that the positive control differs from the negative control only by the additionally adsorbed FhuA vesicles. This procedure ensures that the differential signal between the positive and negative controls is due to specific interactions between the ligands and the FhuA receptors, because vesicles containing non-active FhuA proteins do not bind T5 particles (Fig. 1f).

We verified the coverage of the upper cantilever surface using tapping-mode scanning probe microscopy (atomic force microscopy, AFM). To this end, cantilevers were prepared as described for the binding experiments, and were then washed in water and dried. Figure 3b shows a topography image recorded from a cantilever surface in the centre of the cantilever bar. The

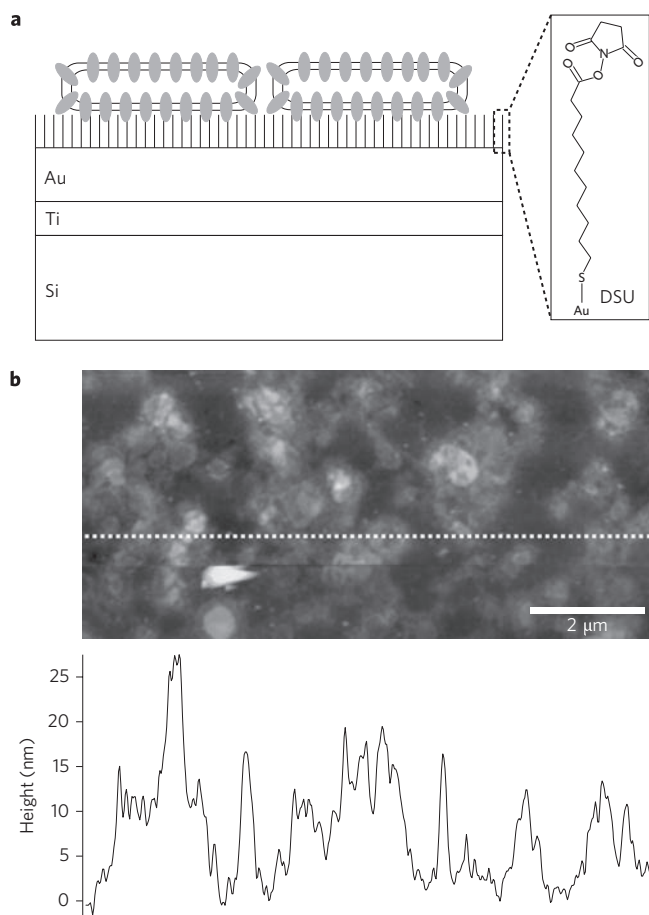


Figure 3 | Functionalization of the upper cantilever surface with FhuA-proteoliposomes. **a**, Schematic of the cantilever functionalization: the gold interface of the cantilever is pre-functionalized with a self-assembling DSU crosslinker, which binds to the gold via a thiol group and reacts by a succinimidyl group with primary amines of FhuA-protein reconstituted in lipid vesicles. **b**, Tapping-mode AFM image of the cantilever surface in the middle of the cantilever bar. The line indicates the position of the recorded height profile shown in the lower panel. FhuA-containing proteoliposomes are clearly visible, similar to the one in Fig. 1a.

measurement reveals typical shapes for FhuA-proteoliposomes, as observed in the TEM images of Fig. 1a. The corresponding AFM height profile along the line indicated in Fig. 3b exhibits height steps of 5 nm, consistent with the thickness of a protein-containing membrane bilayer³³. The ink-jet spotting enabled coverage of the cantilever interface with proteoliposome of at least 64% as estimated by height threshold and particle analysis. Note that a cantilever covered with just casein is able to block unspecific binding (see Supplementary Information, Fig. S5).

Binding mass measurements in dynamic mode

The dynamic mode method is based on measurements of cantilever frequency shifts caused by mass adsorption on the cantilever surface (Fig. 4; see also Methods). The setup enables maximal readout of eight cantilevers in the array in a time-multiplexed manner, which in turn allows a parallel monitoring of the sensing and reference cantilevers in the array. To overcome the large damping of the cantilever movement by the liquid, we performed measurements at higher harmonics, thus improving quality factors³⁴ and sensitivity. We also modelled the amplitude response spectra of the cantilever, not only taking the immediate resonance frequency into account, but also the complete peak region (see Supplementary Information, Fig. S2).

We expect turbulent liquid flow for these frequencies^{34,35}, also providing a good mixing of the injected solution. The functionalized cantilever array was placed into a liquid cell, with the volume of 5 μl filled with binding buffer. All measurements were performed in steady flow at a rate of 10 $\mu\text{l min}^{-1}$ and at a constant temperature of 22 °C.

Figure 5a shows the results of an experiment with T5 virus particles injected for 1 h at a concentration of 3 pM (at a rate of 10 $\mu\text{l min}^{-1}$). Positive control cantilevers (coated with FhuA-proteoliposomes) show evidence of a mass uptake of about 8 ng. These changes are observed within minutes, a performance of the micro-cantilever sensors suited to real-time quantitative bio-applications. In contrast, negative control cantilevers (coated with casein only) show no detectable mass uptake. This observation demonstrates the high specificity of the sensing (FhuA) cantilever for detecting T5 phages, as well as the capability of the casein layer on the reference cantilever to efficiently block unspecific interactions (see Supplementary Information). An additional, independent experiment performed with a solution of T5 virus particles at 1.5 pM shows a mass uptake of about 4 ng (for a 600 μl solution of T5 phages), illustrating the typical reproducibility of our measurements (Fig. 5b). The adsorbed mass remained constant after rinsing the chamber with buffer (similar behaviour was observed at 3 pM), in agreement with previous studies, which have reported an irreversible binding of the T5 virus particles on FhuA^{23,36}.

Finally, in Fig. 5c we present a measurement in which the concentration of T5 virus particles was gradually increased from 30 fM to 3 pM. Here, 600 μl of solution was injected at each concentration. With a typical noise level of ± 0.5 ng, the sensitivity of the instrument was found to be a few hundreds of fM for T5 phages.

Measured bound mass values for T5 bacteriophages are about 8 ng for a 600 μl (3 pM) solution (Fig. 5). This mass uptake was found to be reproducible for independent measurements, correlating with the high quality of the functionalization process (for a total of six independent experiments—using different arrays—at different concentrations, data not shown). Previous studies have shown that T5 phages irreversibly bind to FhuA in a 1:1 molar ratio³⁷. For a 600 μl solution at 3 pM, the total mass of T5 phages ($M_w \approx 7 \times 10^7$ Da) is ~ 130 ng. This means that every ~ 16 th virus particle injected was bound to the sensor interface and that 13% of the accessible FhuA receptors on the cantilever surface were occupied at the end of the experiment (see Supplementary Information; note also that these numbers are roughly calculated from estimated T5 masses and concentrations (plaque-forming units, PFU)). Despite the high efficiency of phage binding, sterical hindrance due to the large virus heads could limit the capacity of the sensor to bind even more particles. The measured mass of the specifically bound phages to the membrane protein receptors is 16 times higher than that calculated for an unspecific binding of hexagonal packed phage heads on the FhuA-functionalized area of the cantilever (64%, Fig. 3b). The phage particles specifically bind, by means of their long and thin tails, to FhuA (Fig. 1d), enabling a three-dimensional arrangement of the phage head. Indeed, TEM studies of phage binding to FhuA-proteoliposomes in solution reveal that the ample tail of the phage enables binding of many more particles on a certain area than the head size allows (see Supplementary Information, Figs S3a, 4). These findings are further proof of the specific binding of the virus particles to their natural receptor *in situ* on the sensor surface.

Conclusions

We have used micro-cantilever arrays to specifically and quantitatively detect bacterial virus particles (T5) interacting with their transmembrane receptors (FhuA) reconstituted in a native state in proteoliposomes. A few reports have demonstrated label-free

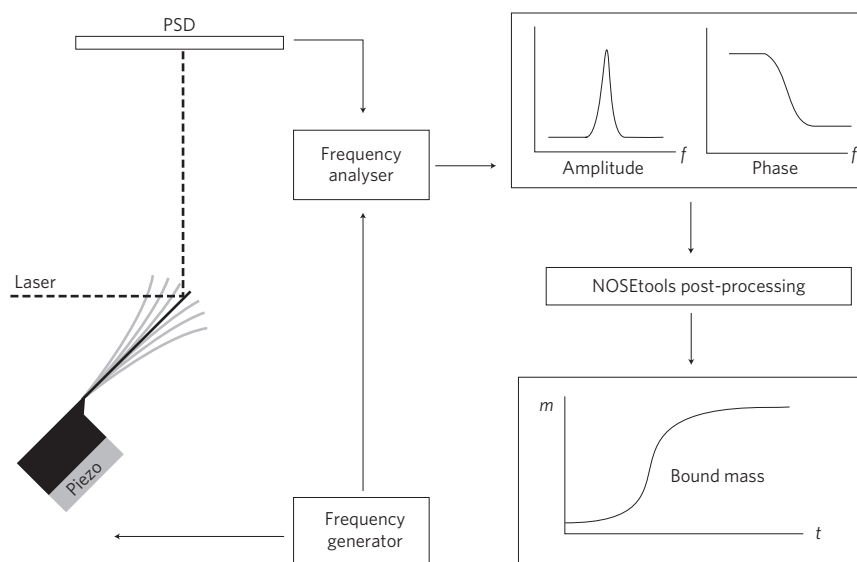


Figure 4 | Schematic of the dynamic-mode measurement setup. A frequency generator sweeps the frequency by exciting a piezoelectric actuator located beneath the base of the microcantilever array. The response of the cantilever is optically detected with a laser using a position-sensitive detector (PSD). The frequency analyser compares the cantilever response with a reference signal from the frequency generator to determine the phase. The amplitude spectrum is recorded with the corresponding phase values. The raw data are analysed by a post-processing software called NOSEtools, which allows the time evolution of the adsorbed mass to be directly determined from the spectrum.

detection using transmembrane proteins^{38,39}, but this is the first time that such studies have been reported in a micro-array format³. This manuscript also presents a novel method (not only applicable to cantilever-based techniques) for functionalization of sensor interfaces with transmembrane proteins.

We used T5 virus particles to validate every step during the sensor preparation with functional membrane proteins (FhuA). The advantage of using reconstituted proteoliposomes is that the transmembrane protein can be stabilized in a native environment directly after purification with a high density of receptor molecules. Furthermore, these vesicles are relatively easy to handle and can be stored. Our data show that the proteoliposomes bind in a native manner to the underlying self-assembled monolayer (DSU crosslinker), either as single membranes or as intact vesicles (see Fig. 3), maintaining the function of the embedded transmembrane protein. The additional protective SAM layer is needed for functional membrane protein receptor immobilization and prevents the membrane proteins from denaturation (Fig. 1e,f).

The measurement technique reported here has not yet been developed to its limits. To increase the sensitivity, we have measured at high modes (modes 10–15)^{18,34,40,41} and fit the amplitude versus frequency spectra using an advanced modelling approach, directly evaluating the mass¹⁸. As we have already demonstrated, this approach is less sensitive to noise than indirectly estimating the mass from the eigenfrequency values¹⁸. Measuring at even higher frequencies and using a quality factor enhancer⁴² could further improve the signal-to-noise ratio. The noise level was found to be to ± 0.5 ng in most of our experiments (using cantilevers of dimensions $500 \mu\text{m} \times 100 \mu\text{m} \times 1 \mu\text{m}$, see Methods), but much smaller noise levels were also sometimes observed. As shown in Fig. 5a, two cantilevers of the same array measured under the same conditions can show variability in measurement noise. This behaviour could be attributed to the current readout system (a vertical-cavity surface-emitting laser composed of eight, non-steerable, lasers¹⁸). Implementing a two-dimensional scanning laser system would allow greater flexibility for choosing optimal positions (such as best reflection, resonance) on each of the cantilevers¹¹. Finally, the ink-jet spotting can also be extended to functionalize both sides of the cantilever, further increasing the concentration sensitivity.

To conclude, microcantilever-based sensors meet the key requirements of a microarray technique: they are small size, they only consume tiny amounts of immobilized material and analyte, and they are capable of multiplexed detection. In the future these sensors might also enable parallel detection of multiple aspects of a binding event, such as mass adsorption (dynamic mode) and conformational changes (static mode). Finally, recent advances in sensor fabrication^{43,44} and deposition techniques⁴⁵ should contribute to the future development of massive parallel cantilever sensors as a tool for label-free and real-time functional microarray analysis³.

Methods

Reconstitution of FhuA in liposomes. FhuA protein overproduced in *E. coli* was solubilized and purified in the detergent *n*-octyl- β -D-glucopyranoside²⁶. FhuA was then complemented with *E. coli* lipid mixture (Avanti polar lipids, product number 100600) using varying lipid-to-protein weight/weight ratios (LPR). The protein–lipid–detergent mixture was dialysed against Tris-buffer (20 mM Tris, 100 mM NaCl, 0.03% NaN₃, pH 8.0) using a continuous flow dialysing device^{27,28}. The proteoliposomes were washed by repeated sedimentation at 12,000 *g* for 20 min at +4 °C and finally resuspended in functionalization buffer (10 mM KH₂PO₄, 50 mM NaCl, 1 mM MgCl₂, 1 mM CaCl₂, pH 8.2).

Phage binding assay in solution. FhuA (3 μg) reconstituted in liposomes was resuspended in 10 μl of binding buffer (20 mM Tris, 100 mM NaCl, 5 mM MgCl₂, 5 mM CaCl₂, pH 8.0), sedimented for 20 min at 12,000 *g* and 4 °C, and resuspended in 15.5 μl binding buffer containing 0.5 μg DNase I and 0.8×10^9 PFU of prepared T5 phages⁴⁶. After incubation for 2 h at room temperature, unbound phage particles were separated from proteoliposome–phage complexes by repeated sedimentation. Phage T5 binding was evaluated by TEM using negative stain.

Phage binding assay on surfaces. Gold-coated cantilever arrays (see below) were immersed in 1 mM solution of di-thio-bis-succinimidyl-undecanoate (DSU, Dojindo)³¹ in water-free dioxan (Fluka) for 1 h, rinsed three times with ethanol, and dried under argon. This step was left out for the negative control without DSU layers. The cantilever arrays were incubated in a proteoliposomes suspension (200 $\mu\text{g ml}^{-1}$ protein in functionalization buffer, see above) and incubated for 1 h at room temperature. After rinsing with the buffer, the plates were incubated in 225 μl binding buffer (see above) containing 8×10^9 PFU of T5 phages for 2 h, rinsed in the buffer and quickly in water, and dried under argon. Platinum (5 nm) was sputtered and the arrays were imaged by SEM.

Functionalization of the cantilever surface. Microfabricated arrays of eight silicon cantilevers (length, 500 μm ; width, 100 μm ; thickness, 1 μm ; spring constant, 0.03 N m⁻¹) from IBM Zurich Research Laboratory were used in all experiments.

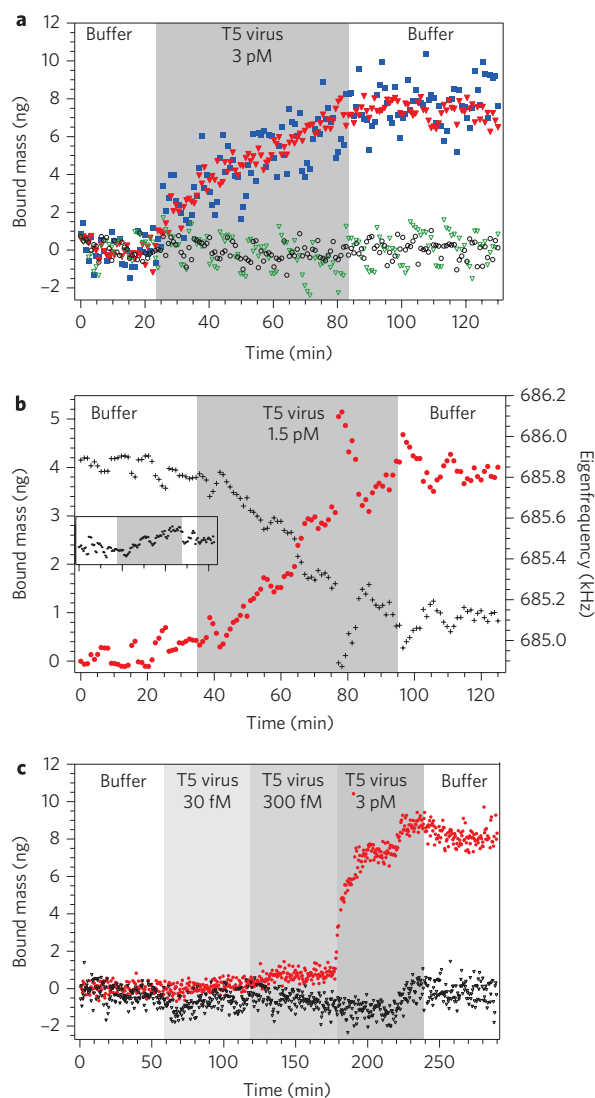


Figure 5 | Docking of T5 phages to FhuA-functionalized cantilevers.

a, A T5 phage solution (3 pM) was injected for 1 h at a rate of $10 \mu\text{l min}^{-1}$. The uptake mass was measured simultaneously on four different cantilevers on one array: two positive controls (FhuA-coated cantilevers, blue squares and red triangles), two negative controls (casein-coated cantilevers, black open circles and green open triangles). Upon the second injection of buffer (after ~ 80 min), the mass uptake remains constant, demonstrating the irreversible binding of T5 phages on FhuA. **b**, The time evolution of the eigenfrequency (14th eigenmode) of the cantilever (the point for which the phase spectrum has its steepest slope) measured for a FhuA-functionalized cantilever ([T5 phages] = 1.5 pM, injected at a rate of $10 \mu\text{l min}^{-1}$, black crosses). Also shown is the corresponding adsorbed mass (red circles). Both the mass and eigenfrequencies are evaluated from a fit of the measured amplitude versus frequency spectra (see Supplementary Information and also ref. 50). The increase in the noise level (at $t = 80$ min) is most probably due to a small air bubble passing in the measurement chamber scattering the laser light. In the inset is shown the response (adsorbed mass) of a negative control cantilever (casein-coated, open circles). **c**, A concentration series experiment, showing the typical sensitivity of the instrument. Red circles and black open triangles indicate the response of the positive (FhuA-coated) and negative (casein-coated) control cantilevers, respectively. At each concentration, a total of $600 \mu\text{l}$ solution (containing the T5 phages) was injected. For all three independent experiments shown here, different arrays were used. (The baseline of the shown experiments here has been adjusted according to ref. 50.).

The arrays were cleaned in Piranha solution (96% H_2SO_4 in 30% H_2O_2 , 1:2) for 10 min, immersed in 30% NH_3 (5 min), rinsed twice with water, and dried in air. The upper sides of the cantilevers were coated with a 2-nm titanium layer (99.99%, Johnson Matthey), followed by a 20-nm gold layer (99.999%, Goodfellow) using an Edwards FL400 electron-beam evaporator (BOC Edwards) at evaporation rates of 0.033 nm s^{-1} (titanium) and 0.07 nm s^{-1} (gold). The gold-coated side of each cantilever was functionalized with a self-assembled monolayer of DSU as described above. FhuA–proteoliposomes (1 mg ml^{-1}) reconstituted in functionalization buffer were dispensed on the pre-functionalized cantilever surface using a modified ink-jet spotting system MDP705L (Microdrop). A humidity chamber maintained the relative humidity at $>95\%$, preventing the sample from drying (Fig. 2). Ten droplets ($\sim 0.1 \text{ nl}$; nozzle size, $70 \mu\text{m}$) were applied on every second cantilever (spot distance, $50 \mu\text{m}$) and incubated for 15 min at 22°C . The array was subsequently rinsed several times with functionalization buffer and incubated for 5 min in 1 mg ml^{-1} of freshly prepared casein solution at room temperature. To dissolve the casein, the protein was agitated at 37°C for at least 2 h before filtering with a $0.2\text{-}\mu\text{m}$ Watson filter. Note that proper preparation of the casein solution is crucial for efficient blocking of the cantilever (see Supplementary Information). Finally, the array was stored in Tris-containing binding buffer (see above) at $+4^\circ\text{C}$. To characterize the functionalization quality, the cantilevers were washed in water and air-dried. Tapping-mode AFM (Nanoscope, Multimode 3a, Veeco) was applied to visualize the FhuA–proteoliposome coverage directly on the cantilever. Imaging cantilevers for tapping mode were purchased from Nanosensors ($k = 40 \text{ N m}^{-1}$). These cantilevers were not used for binding measurements. The image processing and analysis were carried out using Image SXM.

Dynamic-mode mass measurements. A schematic of the setup is shown in Fig. 4. The functionalized cantilever array was installed in the measurement chamber ($5 \mu\text{l}$), filled with binding buffer. A frequency generator was used to periodically excite the piezoelectric actuator placed beneath the cantilever array chip body. The cantilever response was read out using a beam-deflection technique as described in previous work^{18,34,40}. The mechanical response of the cantilever was continuously compared with the excitation wave by a network analyser (Hewlett Packard, 4589A, sweep time of 1 s) that recorded amplitude and the phase spectrum. To increase the sensitivity, we measured at higher modes (modes 10–15)^{18,34,40}. Depending on the number of cantilevers used, a spectrum was recorded every 23 s (for one cantilever) or at least every 3 min for consecutive measurement of all eight cantilevers. During the preparation process, it is possible that some cantilevers are pre-bent and therefore have to be excluded from the measurements. A constant fluid flow rate of $10 \mu\text{l min}^{-1}$ in the cell was maintained using a pressure-driven pump system as described previously⁴⁷. T5 phage solutions were suspended at specific concentrations in binding buffer. Note that we ignore potential stiffening of the cantilever by adsorbed T5 phages. This has been reported for experiments using dried bacteria suspensions in air⁴⁸. However, the current setup is very different from those experiments, and we did not observe significant stiffening effects in experiments with gold layers of precisely controlled thickness⁴⁰.

Data analysis. All data-processing algorithms were implemented in IGOR Pro (www.wavemetrics.com) in a package called NOSEtools^{49,50} (see Supplementary Information).

Data recorded between the 10th and 15th modes were evaluated (post-processing, Fig. 4). For the experiments presented here, the total mass (cantilever, co-moving mass and mass load; see Supplementary Information, equation (3)) was estimated from a fit of the amplitude versus frequency spectra using established theoretical models¹⁸ (see Supplementary Information, equations (5) and (6)). The eigenfrequency (defined as the point at which the phase has its steepest slope) was determined from the total mass (see Supplementary Information, equation (4)). During buffer injection at the beginning of the experiment, the virtual mass co-moving with the cantilever sensor was determined and kept constant for the rest of the experiment. This allowed the mass uptake (induced by binding of the ligands to the cantilevers) to be determined (see Supplementary Information, equation (3)). For all experiments, only one mode was chosen to estimate the mass uptake.

Received 1 September 2008; accepted 3 December 2008; published online 18 January 2009

References

- Howard, A. D. *et al.* Orphan G-protein-coupled receptors and natural ligand discovery. *Trends Pharmacol. Sci.* **22**, 132–140 (2001).
- Cooper, M. Advances in membrane receptor screening and analysis. *J. Mol. Recogn.* **17**, 286–315 (2004).
- Hall, D. A., Ptacek, J. & Snyder, M. Protein microarray technology. *Mech. Ageing Dev.* **128**, 161–167 (2007).
- Hansen, K. M. & Thundath, T. Microcantilever biosensors. *Methods* **37**, 57–64 (2005).
- Lavrik, N. V., Sepaniak, M. J. & Datskos, P. G. Cantilever transducers as a platform for chemical and biological sensors. *Rev. Sci. Instrum.* **75**, 2229–2253 (2004).

6. Fritz, J. *et al.* Translating biomolecular recognition into nanomechanics. *Science* **288**, 316–318 (2000).
7. Backmann, N. *et al.* A label-free immunosensor array using single-chain antibody fragments. *Proc. Natl Acad. Sci. USA* **102**, 14587–14592 (2005).
8. McKendry, R. *et al.* Multiple label-free biodetection and quantitative DNA-binding assays on a nanomechanical cantilever array. *Proc. Natl Acad. Sci. USA* **99**, 9783–9788 (2002).
9. Zhang, J. *et al.* Rapid and label-free nanomechanical detection of biomarker transcripts in human RNA. *Nature Nanotech.* **1**, 214–220 (2006).
10. Mukhopadhyay, R. *et al.* Cantilever sensor for nanomechanical detection of specific protein conformations. *Nano Lett.* **5**, 2385–2388 (2005).
11. Mertens, J. *et al.* Label-free detection of DNA hybridization based on hydration-induced tension in nucleic acid films. *Nature Nanotech.* **3**, 301–307 (2008).
12. Braun, T. *et al.* Conformational change of bacteriorhodopsin quantitatively monitored by microcantilever sensors. *Biophys. J.* **90**, 2970–2977 (2006).
13. Bálint, Z. *et al.* Direct observation of protein motion during the photochemical reaction cycle of bacteriorhodopsin. *Langmuir* **23**, 7225–7228 (2007).
14. Gupta, A., Akin, D. & Bashir, R. Single virus particle mass detection using microresonators with nanoscale thickness. *Appl. Phys. Lett.* **84**, 1976–1978 (2004).
15. Gupta, R., Akin, D. & Bashir, R. Detection of bacterial cells and antibodies using surface micromachined thin silicon cantilever resonators. *J. Vac. Sci. Technol. B* **22**, 2785–2791 (2004).
16. Gfeller, K. Y., Nugaeva, N. & Hegner, M. Rapid biosensor for detection of antibiotic-selective growth of *Escherichia coli*. *Appl. Environ. Microbiol.* **71**, 2626–2631 (2005).
17. Nugaeva, N. *et al.* An antibody-sensitized microfabricated cantilever for the growth detection of *Aspergillus niger* spores. *Microsc. Microanal.* **13**, 13–17 (2007).
18. Braun, T. *et al.* Micromechanical mass sensors for biomolecular detection in a physiological environment. *Phys. Rev. E* **72**, 031907 (2005).
19. Burg, T. P. *et al.* Weighing of biomolecules, single cells and single nanoparticles in fluid. *Nature* **446**, 1066–1069 (2007).
20. Niesters, H. G. M. Molecular and diagnostic clinical virology in real time. *Clin. Microbiol. Infect.* **10**, 5–11 (2004).
21. Poynard, T., Yuen, M. F., Ratziu, V. & Lai, C. L. Viral hepatitis C. *Lancet* **362**, 2095–2100 (2003).
22. Braun, V. & Braun, M. Iron transport and signaling in *Escherichia coli*. *FEBS Lett.* **529**, 78–85 (2002).
23. Böhm, J. *et al.* FhuA-mediated phage genome transfer into liposomes: a cryo-electron tomography study. *Curr. Biol.* **11**, 1168–1175 (2001).
24. Locher, K. P. *et al.* Transmembrane signaling across the ligand-gated FhuA receptor: crystal structures of free and ferrichrome-bound states reveal allosteric changes. *Cell* **95**, 771–778 (1998).
25. Freifelder, D. Molecular weights of coliphages and coliphage DNA. IV. Molecular weights of DNA from bacteriophages T4, T5 and T7 and the general problem of determination of M. *J. Mol. Biol.* **54**, 567–577 (1970).
26. Boulanger, P. *et al.* Purification and structural and functional characterization of FhuA, a transporter of the *Escherichia coli* outer membrane. *Biochemistry* **35**, 14216–14224 (1996).
27. Jap, B. *et al.* 2D crystallization: from art to science. *Ultramicroscopy* **46**, 45–84 (1992).
28. Lambert, O. *et al.* An 8-Å projected structure of FhuA, A 'ligand-gated' channel of the *Escherichia coli* outer membrane. *J. Struct. Biol.* **126**, 145–155 (1999).
29. Lambert, O., Letellier, L., Gelbart, W. M. & Rigaud, J. L. DNA delivery by phage as a strategy for encapsulating toroidal condensates of arbitrary size into liposomes. *Proc. Natl Acad. Sci. USA* **97**, 7248–7253 (2000).
30. Plancon, L. *et al.* Characterization of a high-affinity complex between the bacterial outer membrane protein FhuA and the phage T5 protein pb5. *J. Mol. Biol.* **318**, 557–569 (2002).
31. Wagner, P., Hegner, M., Kernen, F., Zaugg, F. & Semenza, G. Covalent immobilization of native biomolecules onto Au(111) via N-hydroxysuccinimide ester functionalized self-assembled monolayers for scanning probe microscopy. *Biophys. J.* **70**, 2052–2066 (1996).
32. Kenna, J. G., Major, G. N. & Williams, R. S. Methods for reducing non-specific antibody binding in enzyme-linked immunosorbent assays. *J. Immunol. Methods* **85**, 409–419 (1985).
33. Müller, D. J., Amrein, M. & Engel, A. Adsorption of biological molecules to a solid support for scanning probe microscopy. *J. Struct. Biol.* **119**, 172–188 (1997).
34. Ghatkesar, M. K. *et al.* Resonating modes of vibrating microcantilevers in liquid. *Appl. Phys. Lett.* **92**, 3106–3109 (2008).
35. Dorrestijn, M. *et al.* Chladni figures revisited based on nanomechanics. *Phys. Rev. Lett.* **98**, 026102 (2007).
36. Feucht, A., Heinzlmann, G. & Heller, K. J. Irreversible binding of bacteriophage-T5 to its FhuA receptor protein is associated with covalent cross-linking of 3 copies of tail protein-pb4. *FEBS Lett.* **255**, 435–440 (1989).
37. Braun, V. & Endriss, F. Energy-coupled outer membrane transport proteins and regulatory proteins. *Biometals* **20**, 219–231 (2007).
38. Bieri, C., Ernst, O. P., Heyse, S., Hofmann, K. P. & Vogel, H. Micropatterned immobilization of a G protein-coupled receptor and direct detection of G protein activation. *Nature Biotechnol.* **17**, 1105–1108 (1999).
39. Heyse, S., Vogel, H., Sanger, M. & Sigrist, H. Covalent attachment of functionalized lipid bilayers to planar waveguides for measuring protein binding to biomimetic membranes. *Protein Sci.* **4**, 2532–2544 (1995).
40. Ghatkesar, M. K. *et al.* Higher modes of vibration increase mass sensitivity in nanomechanical microcantilevers. *Nanotechnology* **18**, 445502 (2007).
41. Dohn, S., Sandberg, S., Svendsen, W. & Boisen, A. Enhanced functionality of cantilever based mass sensor using higher modes. *Appl. Phys. Lett.* **86**, 233501 (2005).
42. Tamayo, J., Humphris, A. D. & Malloy, A. M. Chemical sensors and biosensors in liquid environment based on microcantilevers with amplified quality factor. *Ultramicroscopy* **86**, 167–173 (2001).
43. Feng, X. L., He, R., Yang, P. & Roukes, M. L. Very high frequency silicon nanowire electromechanical resonators. *Nano Lett.* **7**, 1953–1959 (2007).
44. Despont, M., Drechsler, U., Yu, R., Pogge, H. B. & Vettiger, P. Wafer-scale microdevice transfer/interconnect: Its application in an AFM-based data-storage system. *J. Microelectromech. Sci.* **13**, 895–901 (2004).
45. Bietsch, A., Zhang, J., Hegner, M., Lang, H. P. & Gerber, C. Rapid functionalization of cantilever array sensors by inkjet printing. *Nanotechnology* **15**, 873–880 (2004).
46. Hendrickson, H. E. & McCorquodale, D. J. Genetic and physiological studies of bacteriophage T5 I. An expanded genetic map of T5. *J. Virol.* **7**, 612–618 (1971).
47. Grange, W., Husale, S., Guntherodt, H. J. & Hegner, M. Optical tweezers system measuring the change in light momentum flux. *Rev. Sci. Instrum.* **73**, 2308–2316 (2002).
48. Tamayo, J., Ramos, D., Mertens, J. & Calleja, M. *Appl. Phys. Lett.* **89**, 224104 (2006).
49. Braun, T. *et al.* Digital processing of multi-mode nano-mechanical cantilever data. *J. Phys. Conf. Series* **61**, 341–345 (2007).
50. Braun, T. *et al.* Processing of kinetic microarray signals. *Sens. Act. B* **128**, 75–82 (2007).

Acknowledgements

We thank A. Engel for the use of facilities for protein reconstitution at the Biozentrum, University of Basel, and M. Chami for fruitful discussions. We thank D. Mathys, M. Düggelein and M. Dürrenberger for their help with the SEM analysis. Financial and general support is acknowledged from Swiss National Science Foundation (NCCR Nanoscale Science), the Commission for Technology and Innovation (CTI) (TOPNANO21), the European Learning and Teaching Mobility Regio Network, the G.H. Endress Foundation, the Novartis Foundation and the Science Foundation Ireland CSET programme. M.K.G. thanks the Swiss National Science Foundation and the Novartis Foundation for a research fellowship.

Author contributions

T.B. and M.H. conceived and designed the experiments; T.B. and M.K.G. performed the experiments; T.B., M.K.G., W.G. and M.H. analysed the data; P.B. and L.L. contributed expertise in membrane proteins and phages; A.B. and T.B. were responsible for the ink-jet spotting of the membrane proteins; T.B., N.B., W.G., H.P.L. and M.H. co-wrote the paper. All authors discussed the results and commented on the manuscript.

Additional information

Supplementary Information accompanies this paper at www.nature.com/naturenanotechnology. Reprints and permission information is available online at <http://npg.nature.com/reprintsandpermissions/>. Correspondence and requests for materials should be addressed to M.H.

Supplementary Information:

Quantitative, time-resolved measurement of membrane protein-ligand interactions using microcantilever array sensors

Thomas Braun, Murali Krishna Ghatkesar, Natalija Backmann, Wilfried Grange, Pascale Boulanger, Lucienne Letellier, Hans-Peter Lang, Alex Bietsch, Christoph Gerber and Martin Hegner*

* Corresponding author: Prof. Martin Hegner, CRANN, School of Physics, Trinity College Dublin, Ireland; martin.hegner@tcd.ie

Workflow of the experimental steps needed for the described experiments

A short guide through the complete experimental procedure is presented in **Figure Suppl. 1**. Additionally, more specific information can be found in the manuscript. The FhuA gene was cloned into *E. coli* for over-expression with an engineered His-tag for affinity purification as described before¹ (**panel a**). The membranes were harvested after cell-rupture and were solubilized with the detergent n-octyl- β -D-glucopyranoside¹ (**panel b**). The solubilized FhuA protein was purified on an affinity Ni-NTA-column² (**panel c**). The purified protein was reconstituted in liposomes by mixing it with solubilized lipids and subsequent removal of the detergent by dialysis^{3,4} (**panel d**). Depending of the protein/lipid ratio, the protein was reconstituted as a highly ordered protein array (2D-crystal) or as vesicles (**panel e**, compare with **Fig. 1** of manuscript). To immobilize the proteoliposomes on the cantilever, ink-jet spotting technology combined with a humidity chamber was used (**panel f**, compare with **Fig. 2** and **3** of manuscript). The functionalized cantilever was mounted in the measurement chamber and a solution containing T5-phages was injected. The T5 production was described previously⁵. The frequency response (amplitude and phase) was constantly monitored by a laser detection read-out (**panel g**). These spectra were post-processed using the NOSE-tool software package^{6, 7, 8} to obtain the mass adsorption during the experiment (**panel h**, see **Fig. 4** of manuscript).

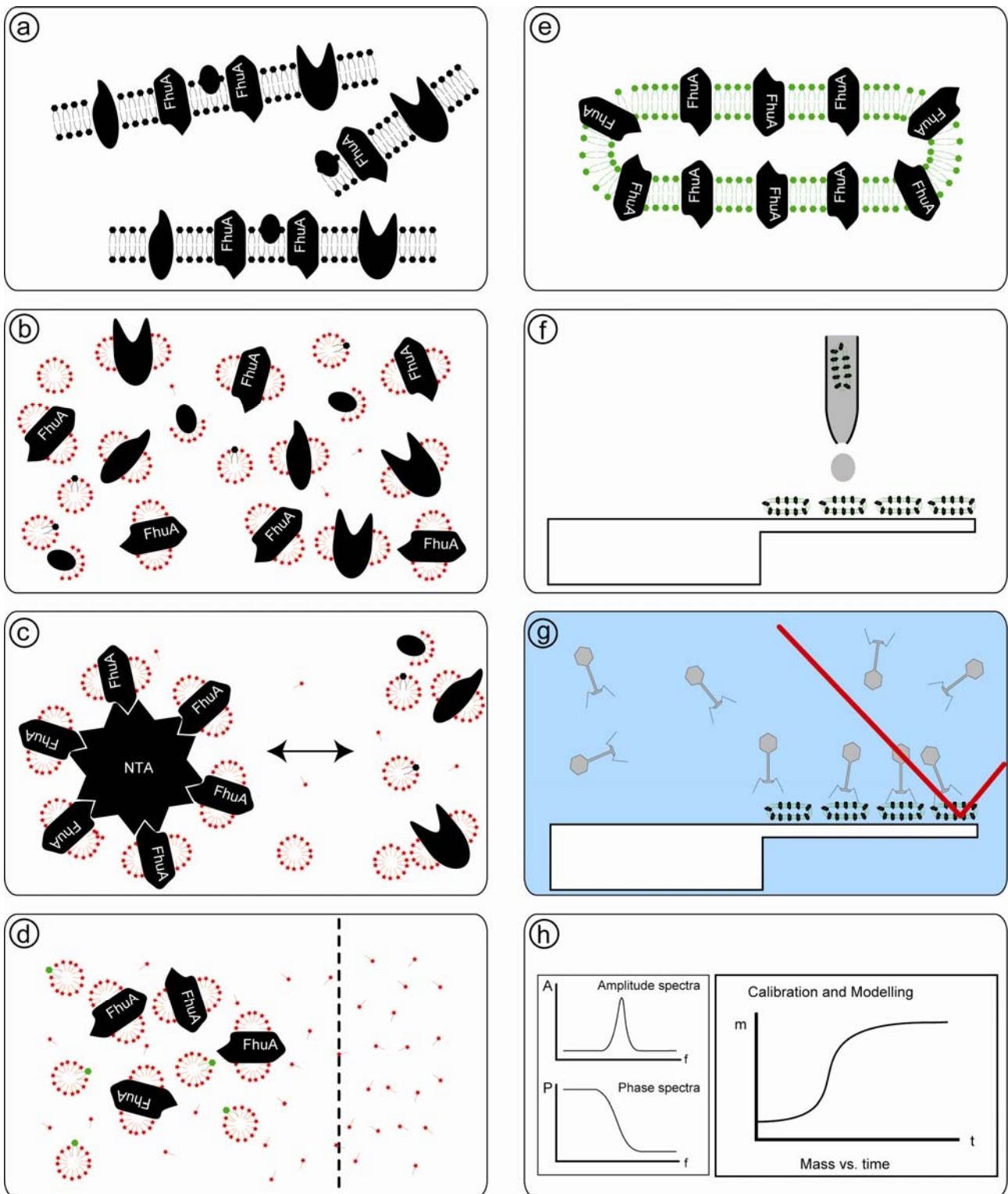


Figure Suppl. 1: Overview over major experimental steps. a) Protein expression of FhuA. b) Solubilization of membranes with detergent (red). c) Affinity purification with an NTA-column. d) Reconstitution of the solubilized FhuA protein in lipid-vesicles by dialysis (green: added lipid). e) Proteoliposome of FhuA vesicles. f) Ink-jet spotting of FhuA proteoliposomes on the upper cantilever interface. g) Phage binding experiment by dynamic mode cantilever sensor. h) Post-processing of recorded spectra (raw-data) to obtain mass changes during experiment.

Theory of the data evaluation

A more detailed discussion about the theory can be found in ref. ⁶, and a description about the NOSEtools software used for data processing is given in ref. ⁷.

The vibration dynamics of a cantilever in vacuum are characterized by the equation of motion, which is given by

$$\underbrace{EI \frac{\partial^4 u(x, t)}{\partial x^4}}_{\text{restoring force}} + \underbrace{C_0 \frac{\partial u(x, t)}{\partial t}}_{\text{intrinsic damping}} + \underbrace{\frac{m_c}{L} \frac{\partial^2 u(x, t)}{\partial t^2}}_{\text{inertial force}} = 0 \quad (1)$$

EI is the flexural rigidity of the cantilever spring. E is the Young's modulus and I the moment of inertia. C_0 is the intrinsic damping coefficient per unit length that describes internal losses; m_c is the mass of the cantilever and L the length of the cantilever. $U(x; t)$ is the deflection of the cantilever perpendicular to the cantilever axis. X is the coordinate along the cantilever axis and t is time.

For cantilevers vibrating in a liquid environment and driven by a piezoelectric crystal plate, three additional forces have to be taken into account: First, the motion of the cantilever experiences an additional resistance, because not only the cantilever, but also a specific amount of the fluid has to be accelerated. This means that the surrounding fluid acts on the cantilever as if an additional mass m_l is attached to the cantilever. This commoving mass is also called 'virtual mass'. Second, an additional dissipative force per unit length acts on the cantilever that is proportional to the velocity, $g_v = -C_v \frac{\partial u(x, t)}{\partial t}$, where C_v is the external dissipation coefficient. Third, an external periodic force per unit length acts on the cantilever ($F(x; t)$). Taking these three additional forces into account, Eq. (1) can be expanded to

$$EI \frac{\partial^4 u(x, t)}{\partial x^4} + \underbrace{C_v \frac{\partial u(x, t)}{\partial t}}_{\text{external damping}} + C_0 \frac{\partial u(x, t)}{\partial t} + \underbrace{\frac{m_l}{L} \frac{\partial^2 u(x, t)}{\partial t^2}}_{\text{inertial force of "virtual mass"}} + \frac{m_c}{L} \frac{\partial^2 u(x, t)}{\partial t^2} = \underbrace{F(x, t)}_{\text{periodic driving force}} \quad (2)$$

In this study we detect an uptake of tiny amounts of mass distributed over the entire cantilever that is due to ligand-receptor interaction on the cantilever surface. Therefore, this additional mass must be taken into account in all formulas above for the total mass:

$$m_{\text{total}} = m_c + m_l + \underbrace{\Delta m}_{\text{mass load}} \quad (3)$$

Equation 2 can be solved for a rectangular cantilever with evenly distributed mass load to describe the recorded frequency spectra for the amplitude and phase. The eigenfrequency f_{0n} of the cantilever in mode n is given as follows:

$$f_{0n} = \frac{\alpha_n^2}{2\pi} \sqrt{\frac{k}{3(m_{\text{tot}})}} \quad (4)$$

k is the cantilever constant ($k = 3EI/L^3$). The α_n are related to the different eigenvalues of the harmonics and are fixed by the boundary conditions⁹. ($\alpha_1 = 1.875$, $\alpha_2 = 4.694$, $\alpha_3 = 7.854$, $\alpha_4 = 11.0$, $\alpha_{5..n} = \pi(n-0.5)$.)

The amplitude of the response of the n th harmonics in dependence of the frequency of the driving force f is given according to the model of a damped harmonic oscillator by

$$u_n(f) = \frac{u_{\text{max}} f_{0n}^2}{\sqrt{(f_{0n}^2 - f^2)^2 + \frac{\gamma^2 f^2}{\pi^2}}} \quad (5)$$

The damping factor γ is defined by

$$\gamma = \frac{C_0 + C_v}{\frac{2}{L} m_{\text{tot}}} \quad (6)$$

In our case the damping factor is dominated by the liquid .

The function 5 is also called resonance curve and has a maximum at the peak-frequency

$$f_n = \sqrt{f_{0n}^2 - \frac{\gamma^2}{2\pi}} \quad (7)$$

The phase between response and driving force in dependence of the frequency of the driving force is given by:

$$\varphi(f) = \arctan \frac{-\gamma f}{\pi(f_{0n}^2 - f^2)} \quad (8)$$

The eigenfrequency f_{0n} is defined as the point where the phase curve has its steepest slope. For the phase spectra, the damping γ only affects the slope around the eigenfrequency but not the position in the spectra. In contrast to that, the amplitude peak gets broader (lower Q factor) and the peak-frequency is shifted towards lower values. Note that the external damping dominates the system in liquid⁶.

In order to determine the mass load Δm , the virtual mass m_i must be determined at the beginning of the experiment (calibration). The external damping C_v is always defined by the amplitude peak width and the peak-frequency or by the gradient around the phase turn-point respectively.

Experimental data analysis

As mentioned in the **Materials and Methods** section, the total mass was estimated from a fit of the amplitude *versus* frequency spectra (Eq. 5) (**Figure Suppl. 2**). The relation between the total mass and the eigenfrequency (damping coefficient) was given by Eq. 4 (Eq. 6). The ‘virtual mass’ as well as the mass of the cantilever were calibrated at the beginning of the measurement and then was kept constant over the experiments^{10, 8}. For the experiment presented in the manuscript, only one peak of the amplitude spectrum was fitted.

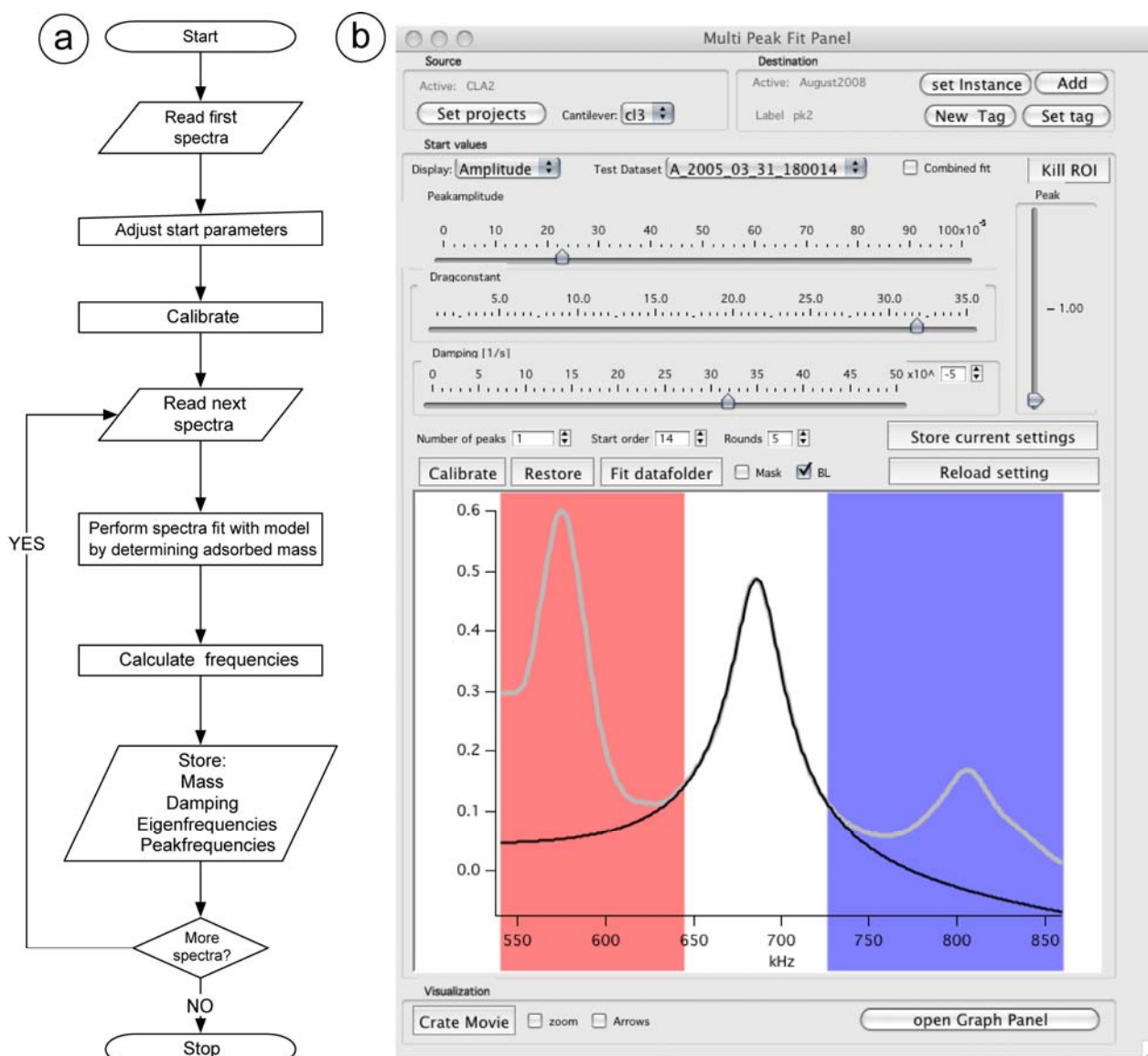


Figure Suppl. 2: Simplified flow diagram for peak tracking and model fit algorithms. a) Work flow for mass determination by modelling a series of spectra. b) Graphical user interface for data modelling. Note the preview-window with the raw data (thick grey line) and the model fit in black.

In situ reference cantilevers

When planning differential nano-mechanical cantilever array experiments, the choice of the reference cantilever functionalization is certainly one of the most crucial issues. For measurements involving the binding of T5 on FhuA receptors, cantilevers coated with casein only were found to be ideal negative controls (see also **figure suppl. 5**) due to the absence of non-specific binding on the positive control cantilevers (FhuA coated) when the FhuA is inactivated (**figure 1f** and **figure suppl. 3a**). The situation might be different when also non-specific interactions on the positive control cantilevers are likely to occur.

To illustrate this behavior, we have performed nano-mechanical experiments involving the binding of ferrichrome (MW 687.7 Da), an iron-chelating molecule, which allows the translocation of iron across FhuA channels¹¹. **Figure suppl. 3c** shows the result of a binding experiment of the small ligand ferrichrome to FhuA functionalized membrane protein cantilevers. Here, similar positive and negative control cantilevers as for experiments involving T5 where used. Considering the number of active and accessible FhuA sites on the cantilevers (5.3×10^8), the expected mass uptake is smaller than 1 pg, much smaller than our current detection limit of our apparatus (~ 0.5 ng). After recording the baseline in buffer, ferrichrome was injected at a concentration of $1 \mu\text{M}$, slightly above its dissociation constant¹². While the casein reference cantilever¹² does not show a mass uptake during the injection of ferrichrome [$600 \mu\text{l}$ of a [$1 \mu\text{M}$] solution ($10 \mu\text{l}/\text{min}$)], the positive control cantilever (membrane-FhuA functionalized) evidence for a mass uptake of about 2 ng (**figure suppl. 3c**). This non-specific binding (found to be reproducible for three independent measurements performed on different arrays) is attributed to electrostatic interactions between the lipid head groups and the negatively charged ferrichrome molecules (**figure suppl. 3b**). In summary it remains a major challenge for surface based techniques (cantilevers, surface plasmon resonance¹³, quartz crystal microbalance¹⁴ (QCM)) to elucidate specific binding kinetics of small ligands.

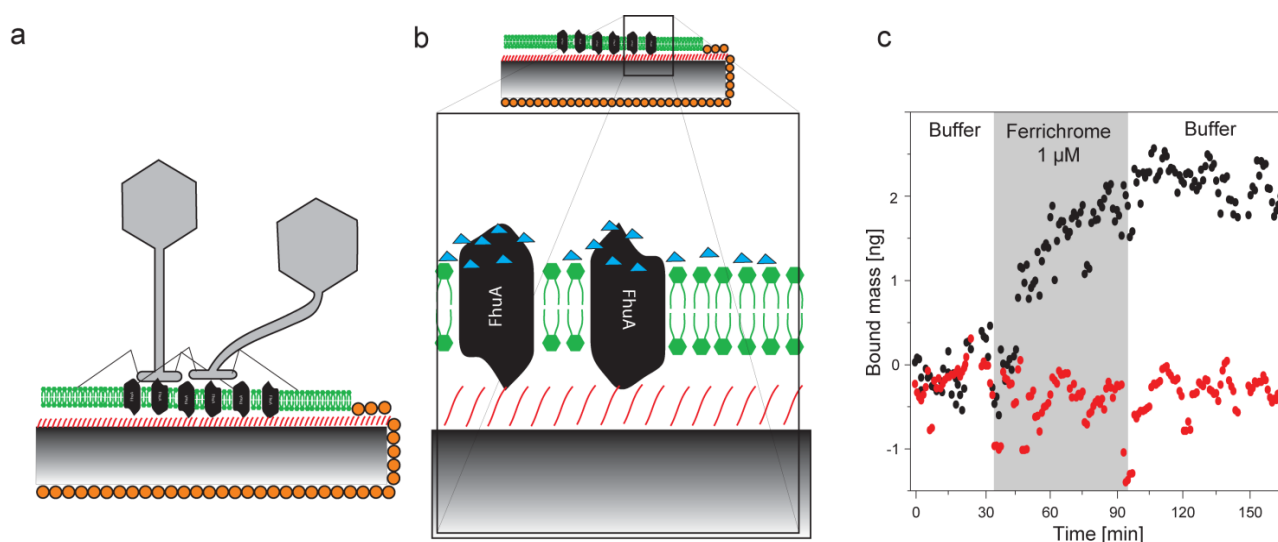


Figure Suppl. 3: Ligand binding on native membrane protein functionalized microcantilever. T5 virus (grey hexagonal structures), lipid bilayer (green), FhuA trans-membrane protein (black), self-assembled hetero-bifunctional monolayer (red), Cantilever (black-grey, not drawn to scale), casein (orange), ferrichrome (blue triangle). a) Specific binding of T5 virus to FhuA membrane protein. No binding is observed on casein protected interfaces nor on lipid area depleted from FhuA (or having non-active FhuA receptors, **figure 1f**). b) Binding of ferrichrome to the FhuA membrane proteins and the lipid bilayer. No binding is observed on casein protected interfaces but non-specific interactions occur between ferrichrome and the lipid bilayer.

c) Binding of ferrichrome to FhuA membrane protein functionalized sensor (black dots), casein blocked reference cantilever (red dots).

Phage load of FhuA containing vesicles

The long tail of T5 provides an ample flexibility between the anchoring point of the phage and the DNA containing head as demonstrated by the following image (see also **fig. suppl. 3a**). The binding experiment was performed as described above in the presence of 100 nM ferrichrome.

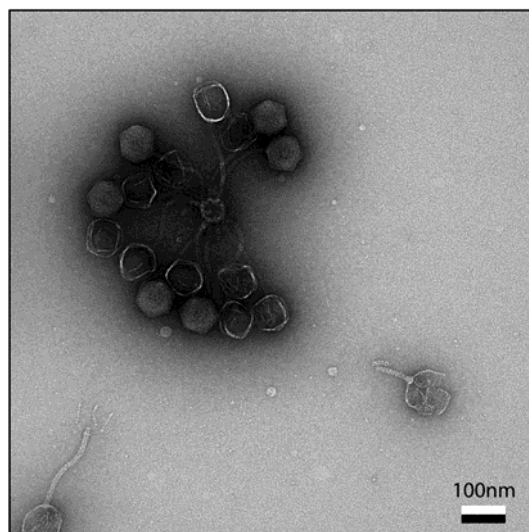


Figure Suppl. 4: TEM image of T5 virus binding to a small proteoliposome which was pre-incubated with 100 nM ferrichrome. The small proteoliposome in the middle is surrounded by T5 phage particles.

Cantilever functionalization

Throughout the functionalization process, the variability of the FhuA protein (receptor) density was minimized. As such, the binding experiments presented in the manuscript (**Figure 5**) show a good repeatability. We mention, however, both the preparation of the reconstituted FhuA membrane receptors and the functionalization of sensing cantilevers is a demanding task.

The FhuA must be reconstituted in proteoliposomes due to the nature of the amphiphilic membrane protein. We used a flow-controlled machine originally developed for 2D crystallization³. One assay contained maximally 50 μ l as start volume; however, due to loss of material and osmotic/flow pressure effects only 30 μ l are recovered at the end. Since in every protein purification the amount of associated lipids with the protein varies, we performed the reconstitution preparations always with a series of different lipid-protein ratio. Therefore, only a limited amount of experiments can be performed with one sample. Densely packed to mosaic crystalline vesicles gave good results with phage binding, whereas high crystalline sheets did not show activity if adsorbed on cantilever surfaces. The application of an ink-jet spotting device (using pico-liter droplets as shown in **Figure**

2 of the manuscript) is still enabling many experiments with one batch and reduces the amount of material used for the functionalization. Note, however, that a standard micro-capillary functionalization procedure can be used for other experiments (genomics, soluble proteins)^{15, 16}.

Specificity of binding and blocking of unspecific binding by casein

We examined also the underside of the ink-jet functionalized cantilevers by tapping mode AFM (as in **Figure 3** of manuscript). Only a very small amount of proteoliposomes structures were observed, most probably from the first washing step after functionalization with the ink-jet spotter, which selectively wets the upper cantilever surface with the proteoliposome solution. This is in good agreement with bacteriorhodopsin experiments performed previously¹⁷. We also made control experiments for unspecific phage adsorption on the cantilever backside and could only find few phage particles (maximally 1 to 2 phage head/ μm^2 , **figure suppl. 5**). However, casein could form inhomogeneous micellular structures which grow with time¹⁸ and might look very similar to T5 Phages in the AFM¹⁹ which could complicate the interpretation but none were found when fresh casein was used.

The cantilever was functionalized as described in the manuscript and the array was incubated for 1.5h in a solution containing 20mM Tris HCL pH 8, 5mM MgCl_2 , 5mM CaCl_2 , 100mM NaCl, 0.01% NaN_3 and 0.2pM PFU of T5 phages. Arrows indicate regions which could be interpreted as adsorbed virus particles.

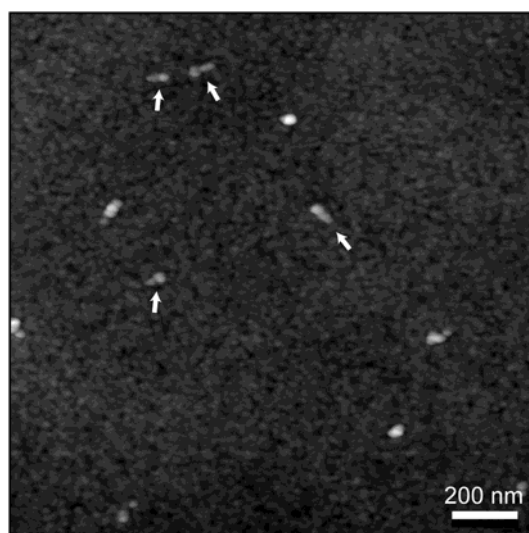


Figure Suppl. 5: AFM image of the backside of cantilevers passivated with casein and incubated for 1.5h in a solution of 0.5pM T5 solution (arrows mark either T5 phages or possible casein aggregates) Note that the conditions here are different from the in-situ experiments presented in the manuscript.

We performed EM experiments with casein which could form micelles when stored over time and negative stain similar to the EM pictures performed in **figure 1** of the manuscript. However, the surface structure and charge are different than the situation *in situ* on the cantilever.

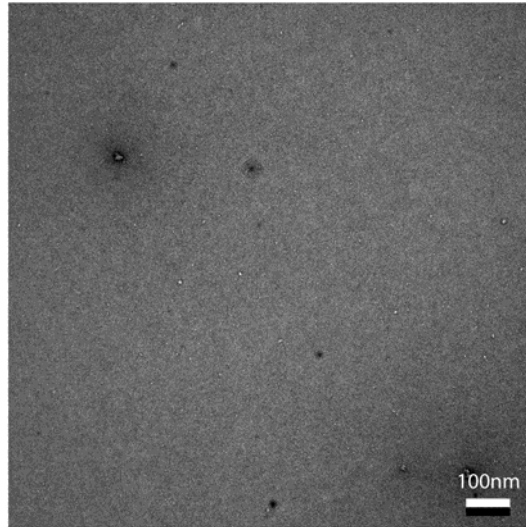


Figure Suppl. 6: Casein adsorbed on glow-discharged EM grid in negative stain (protein white). A fresh solution of nominal 1mg/ml casein (filtered with 0.2 μ m filter) was incubated for 1 min on a 20s glow discharged EM carbon-palladium grid and stained for 2x12sec with 2% Uranyl acetate.

The estimated density of unspecific T5 particles is around 1 to 2 particles/ μ m². We would like to point out, that viruses must avoid unspecific binding to be successful in nature.

Calculation of maximal bound FhuA virus to the cantilever

Input parameters are in *italic*. Note that these calculations are rough estimations and ignore the spherical nature of the proteoliposomes significantly enlarging the active sensor surface.

Number of FhuA receptors on cantilever		
	Value	Unit
<i>Coverage of cantilever with FhuA patches</i>	64%	
<i>Unit cell axis a</i>	12.4	nm
<i>Unit cell axis b</i>	9.8	nm
<i>Number of FhuA molecules per unit cells</i>	4	
<i>Symmetry related accessibility (p22₁2₁)</i>	0.5	
Cantilever width	100	μ m
Cantilever length	500	μ m
Area of cantilever	50000	μ m ²

Area per FhuA molecule	0.00003038	μm^2
Minimal number of FhuA molecules on cantilever	1.1E+9	molecules
Minimal number of accessible FhuA on cantilever	5.3E+08	molecules

Table Suppl. 1: Structural information from Lambert et al. ⁴. P22₁2₁ symmetry assumed, or densely packed vesicle: Therefore only every second FhuA molecule will be accessible. This does not take double layers (vesicles) into account and ignores the spherical nature of the used proteoliposomes.

Number of T5 heads on cantilever		
	Value	Unit
<i>Head size of phage</i>	~75	nm
<i>Unit cell of hexagonal arrangement</i>	14614.2	nm^2
<i>Number per unit cell</i>	2	phages
Cantilever width	100	μm
Cantilever length	500	μm
Coverage of cantilever with FhuA patches	64	%
Number of densely packed phage heads on the cantilever (if unspecifically physisorbed)	6.84E+06	phages
Number of densely packed phage heads on FhuA functionalized cantilever areas	4.38E+06	phages

Table Suppl. 2: Estimation of maximal phage bound to the cantilever due to the head size of the T5-virus. Unspecific binding and hexagonal packing of the head is assumed.

Comparison with experiment		
	Value	Unit
<i>Measured mass</i>	~8	ng
<i>Mass per phage</i>	7.0E+07	Da
<i>Mass per phage</i>	1.2 E-07	ng
Number of measured phages	6.7 E+07	phages
Phage head packing ratio (measured specifically bound / calculated for unspecific adsorption)	15	
Percentage of occupied FhuA receptors	13%	occupation rate

Table Suppl 3: Phage mass calculations using the reported mass of Freifelder et al. (1970)²⁰. *Phage head packing ratio:* Number of densely packed heads on the cantilever divided by the measured head phage number. *Percentage of occupied FhuA receptor:* FhuA Molecules with bound phages relative to the total amount of FhuA receptors.

References

1. Boulanger, P. et al. Purification and structural and functional characterization of FhuA, a transporter of the Escherichia coli outer membrane. *Biochemistry* **35**, 14216-14224 (1996).
2. Hochuli, E., Dobeli, H. & Schacher, A. New metal chelate adsorbent selective for proteins and peptides containing neighbouring histidine residues. *J. Chromatogr.* **411**, 177-184 (1987).
3. Jap, B. et al. 2D Crystallization: From Art to Science. *Ultramicroscopy* **46**, 45-84 (1992).
4. Lambert, O. et al. An 8-A projected structure of FhuA, A "ligand-gated" channel of the Escherichia coli outer membrane. *J. Struct. Biol.* **126**, 145-155 (1999).
5. Hendrickson, H.E. & McCorquodale, D.J. Genetic and Physiological Studies of Bacteriophage T5 I. An Expanded Genetic Map of T5. *J. Virol.* **7**, 612-618 (1971).
6. Braun, T. et al. Micromechanical mass sensors for biomolecular detection in a physiological environment. *Phys. Rev. E* **72**, 031907 (2005).
7. Braun, T. et al. Digital Processing of Multi-Mode Nano-Mechanical Cantilever Data. *J. Phys. Conf. Series* **61**, 341-345 (2007).
8. Braun, T. et al. Processing of kinetic microarray signals. *Sens. Act. B* **128**, 75-82 (2007).
9. Young, D. & Felgar Tables of Characteristic Functions Representing Normal Modes of Vibration of a Beam. *The University of Texas Publication* **44**, 1-32 (1949).
10. Braun, T., Kaufmann, T., Remigy, H. & Engel, A. in *Encyclopedic Reference of Genomics and Proteomics in Molecular Medicine*. (ed. D.R. Ganten, Klaus)2005).
11. Faraldo-Gomez, J.D. & Sansom, M.S.P. Acquisition of siderophores in Gram-negative bacteria. *Nature Rev. Mol. Cell Biol.* **4**, 105-116 (2003).
12. Locher, K.P. & Rosenbusch, J.P. Oligomeric states and siderophore binding of the ligand-gated FhuA protein that forms channels across Escherichia coli outer membranes. *Eur. J. Biochem.* **247**, 770-775 (1997).
13. Alves, I.D., Park, C.K. & Hruby, V.J. Plasmon resonance methods in GPCR signaling and other membrane events. *Curr. Protein Pept. Sci.* **6**, 293-312 (2005).
14. Zilberman, G. & Smith, A.L. QCM/HCC as a platform for detecting the binding of warfarin to an immobilized film of human serum albumin. *Analyst* **130**, 1483-1489 (2005).
15. Zhang et al. Rapid and label-free nanomechanical detection of biomarker transcripts in human RNA. *Nature Nanotech.* **1**, 214-220 (2006).
16. Backmann, N. et al. A label-free immunosensor array using single-chain antibody fragments. *Proc. Natl. Acad. Sci. USA* **102**, 14587-14592 (2005).
17. Braun, T. et al. Conformational change of bacteriorhodopsin quantitatively monitored by microcantilever sensors. *Biophys. J.* **90**, 2970-2977 (2006).
18. Pignon, F. et al. Structure and rheological behavior of casein micelle suspensions during ultrafiltration process. *J. Chem. Phys.* **121**, 8138-8146 (2004).
19. Gebhardt, R., Doster, W., Friedrich, J. & Kulozik, U. Size distribution of pressure-decomposed casein micelles studied by dynamic light scattering and AFM. *Eur. Biophys. J.* **35**, 503-509 (2006).
20. Freifelder, D. Molecular weights of coliphages and coliphage DNA. IV. Molecular weights of DNA from bacteriophages T4, T5 and T7 and the general problem of determination of M. *J. Mol. Biol.* **54**, 567-577 (1970).